JOURNAL OF GEOPHYSICAL RESEARCH, VOL. 112, B05422, doi:10.1029/2006JB004367, 2007

Improving the precision of high-rate GPS

Kristine M. Larson,[1] Andria Bilich,[1] and Penina Axelrad[1]

Received 28 February 2006; revised 10 October 2006; accepted 28 December 2006; published 31 May 2007.

[1] In order to improve the accuracy of high-rate (1 Hz) displacements for geophysical applications such as seismology it is important to reduce systematic errors at seismic frequencies. One such GPS error source that overlaps with seismic frequencies and is not currently modeled is multipath. This study investigates the frequencies and repetition of multipath in high-rate GPS time series in order to maximize the effectiveness of techniques relying upon the geometric repeatability of GPS satellite orbits. The implementation of the aspect repeat time adjustment (ARTA) method described here uses GPS position time series to estimate time-varying and site-dependent shifts. As demonstrated for high-rate GPS sites in southern California this technique significantly reduces positioning noise at periods from 20 to 1000 s. For a 12-hour time series, ARTA methods improve the standard deviation of the north component from 8.2 to 5.1 mm and the east component from 6.3 to 4.0 mm. After applying ARTA corrections, common mode errors are removed by stacking. This method further improves the standard deviations to 3.0 and 2.6 mm for the north and east components, respectively.

Citation: Larson, K. M., A. Bilich, and P. Axelrad (2007), Improving the precision of high-rate GPS, *J. Geophys. Res.*, *112*, B05422, doi:10.1029/2006JB004367.

1. Introduction

[2] Our understanding of earthquakes requires first constraining the kinematic and dynamic models of fault rupture. The ability to resolve ground motions accurately over a range of frequencies and amplitudes is critical to understanding these processes. Several methods exist for resolving ground motions, each with inherent strengths and limitations. Accelerometers, for example, capture the details of strong ground shaking near the source, but it is difficult to convert the acceleration measurements unambiguously to displacement. These problems are compounded for long periods or when the accelerometer experiences strong or permanent rotations. Broadband seismometers are more sensitive and have better resolution of ground motion but may clip, saturate, or become nonlinear even to great distances from a large earthquake. Interferometric synthetic aperture radar (InSAR) observations can produce spatially rich images of some components of surface displacement surrounding a rupture, but InSAR is prone to failure in certain regions and has insufficient temporal resolution to resolve short-term dynamic changes during an earthquake. GPS instrumentation has been important in earthquake studies for resolving coseismic offsets, which places important constraints on the rupture process, but until recently, GPS observations were not sampled frequently enough to measure ground displacements associated with earthquake rupture.

[3] An increasing number of continuously operating GPS receivers originally installed for long-term geophysical studies are now operating at seismic frequencies, e.g., 1 Hz. In situ experiments and comparative studies described by *Ge* [1999] and *Ge et al.* [2000a] indicate that high-rate GPS can resolve large displacements in a short-baseline environment. More recently, new studies have shown good agreement between seismic and (1 Hz) high-rate GPS measurements [*Elósegui et al.*, 2006; *Wang et al.*, 2007; *Emore et al.*, 2007]. *Larson et al.* [2003] used 1-Hz GPS to observe large ground motions over continental scales during the Denali Fault earthquake; *Bock et al.* [2004] showed relative measurements from southern California for the same event. Following the Denali event, high-rate GPS data began to be used in seismic rupture studies [*Ji et al.*, 2004; *Miyazaki et al.*, 2004; *Langbein et al.*, 2005; *Kobayashi et al.*, 2006] for earthquakes ranging in magnitude from *M*6 to 8. The high-rate GPS technique builds on the basic tools and developments used in traditional GPS analysis: precise orbits in a well-defined terrestrial reference frame, an expanded constellation of 29 GPS satellites providing greater global coverage, and high-precision geodetic software. Unlike geophysical studies that average many GPS observations to compute one position per day [*Segall and Davis*, 1997], high-rate GPS analyses compute one position per epoch; precision is therefore strongly affected by systematic errors. For high-rate GPS applications such as seismology, methodologies must be developed to reduce the influence of systematic errors such as multipath on GPS position estimates. This paper describes how multipath effects vary in GPS time series and describes methods for removing these effects. We sub-

[1]Department of Aerospace Engineering Sciences, University of Colorado, Boulder, Colorado, USA.

0148-0227/07/2006JB004367$09.00

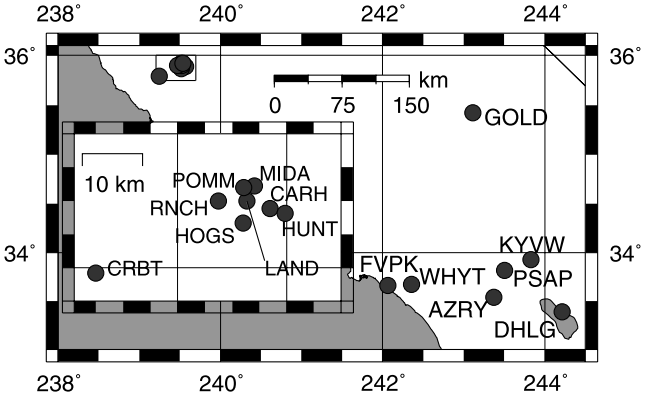

Figure 1. GPS stations used in this study. There is a small cluster of sites at Parkfield (shown in the inset). Further description of the sites is available at http://www.scign.org.

sequently assess the precision of high-rate GPS at periods of 2–1000 s.

2. GPS Data Analysis

[4] The analysis of high-rate GPS data is common in real-time applications associated with navigation, surveying, and structural monitoring. There are also a growing number of high-rate GPS publications in the geophysical literature [*Celebi et al.*, 1999; *Bock et al.*, 2000; *Melbourne and Webb*, 2002]. Software developed for high-rate geophysical applications makes use of many of the same models used for 24-hour averages, but the estimation strategies are more varied. For example, when 24-hour average positions are computed, most geodetic software estimates one phase ambiguity per satellite station arc [*Blewitt*, 1989]. This can also be done in high-rate GPS studies [*Larson et al.*, 2003]. In the high-rate positioning analysis strategy described by *Bock et al.* [2000] a new phase ambiguity is estimated at every data epoch. Subsequently, ambiguity resolution is attempted. One benefit of this strategy is that it obviates the need to detect cycle slips; the weakness of the strategy is that positions will be very poorly determined if ambiguity resolution is not successful. Demonstrations of this implementation of high-rate positioning [e.g., *Mattia et al.*, 2004] have largely been limited to baselines less than 20 km. *Kouba* [2003] describes a high-rate analysis strategy that uses the International Global Navigation Satellite Systems (GNSS) Service (IGS) precise orbit and clock products [*Beutler et al.*, 1994; http://igscb.jpl.nasa.gov]. While *Bock et al.* [2000] double differences carrier phase observables to remove clock errors, *Kouba* [2003] interpolates from 5-min IGS satellite clock values and estimates the receiver clock. *Kouba*'s [2003] strategy is computationally efficient; because the data from each receiver are analyzed separately, there is no restriction on baseline length.

[5] In this study the GPS Inferred Positioning System (GIPSY) software is used to analyze the GPS data [*Lichten and Border*, 1987]. The IGS precise orbits, defined in International Terrestrial Reference Frame 2000 (ITRF2000), are used to define the coordinates of the GPS satellites [*Beutler et al.*, 1994]. One station is used as the reference; its position is constrained (a priori standard deviation of 1 cm) to agree with its ITRF2000 position [*Altamimi et al.*, 2002]. Although in theory any station in the network can be used as the reference site, any motion at that site (e.g., static or dynamic seismic displacements) must be accounted for in the processing software; otherwise, all high-rate positions in the network will become relative positions (corrupted by the reference site's motion) rather than absolute positions. For all other sites, positions in a local coordinate system (east, north, and vertical) are estimated every second with a loose a priori constraint (100 m). Other estimated parameters include satellite and receiver clocks, constant zenith troposphere delays, and carrier phase ambiguities. Ambiguities are resolved using the methods described by *Blewitt* [1989]. In this paper, only horizontal component precision will be discussed; high-rate GPS vertical positions are left for future work. Because of GIPSY software constraints, only 3.3-hour time segments will be analyzed in one batch.

[6] These analysis methods will be applied to data from continuously operating GPS sites in southern California to assess the positioning noise characteristics of individual sites and the network as a whole. The sites (Figure 1) are part of the Southern California Integrated GPS Network (SCIGN) [*Hudnut et al.*, 2002]. This subset of SCIGN sites operates at 1 Hz. All use a common receiver/antenna (ASHTECH Z-XII3/choke-ring antenna) and many have a similar monument design (drill braced with radome). Many of the sites analyzed here were previously discussed by *Langbein and Bock* [2004]. We focus on high-rate GPS data collected in the days before and after the Parkfield earthquake, 28 September 2004, 1715 UTC.

[7] Figure 2 illustrates the variation in noise characteristics for a few of the high-rate GPS sites included in this study. Spectrograms (time-varying power spectra) are shown for the north component for three SCIGN stations and one IGS site (GOLD). As will be shown in section 6, east components are better determined than north components but have similar variation in noise characteristics. Except at the highest frequencies the noise spectra follow a power law relationship, i.e., $\sim$1/frequency [*Agnew*, 1992]. In addition to these common characteristics each of these GPS sites exhibits unique noise characteristics. CRBT and POMM have low power at short periods and higher power at long periods but exhibit transient noise at very short periods (25–50 s) at different times. Conversely, GOLD noise has more power at short periods (30–100 s) and less power at longer periods. As previously noted [*Langbein and Bock*, 2004], MIDA has significantly more noise at longer periods (300–3000 s) than any of the other sites in this network.

[8] Because the same satellites, receiver types, and software were used to compute positions at each site, the differences in noise characteristics must be generated by something specific to the individual GPS sites. In section 3 we will show that these noise characteristics at CRBT, POMM, GOLD, and MIDA are consistent with errors due to multipath and can be related to the location of the antenna with respect to reflecting surfaces. We summarize the mathematical formulation needed to relate the frequency of high-rate GPS errors to the local multipath conditions at a

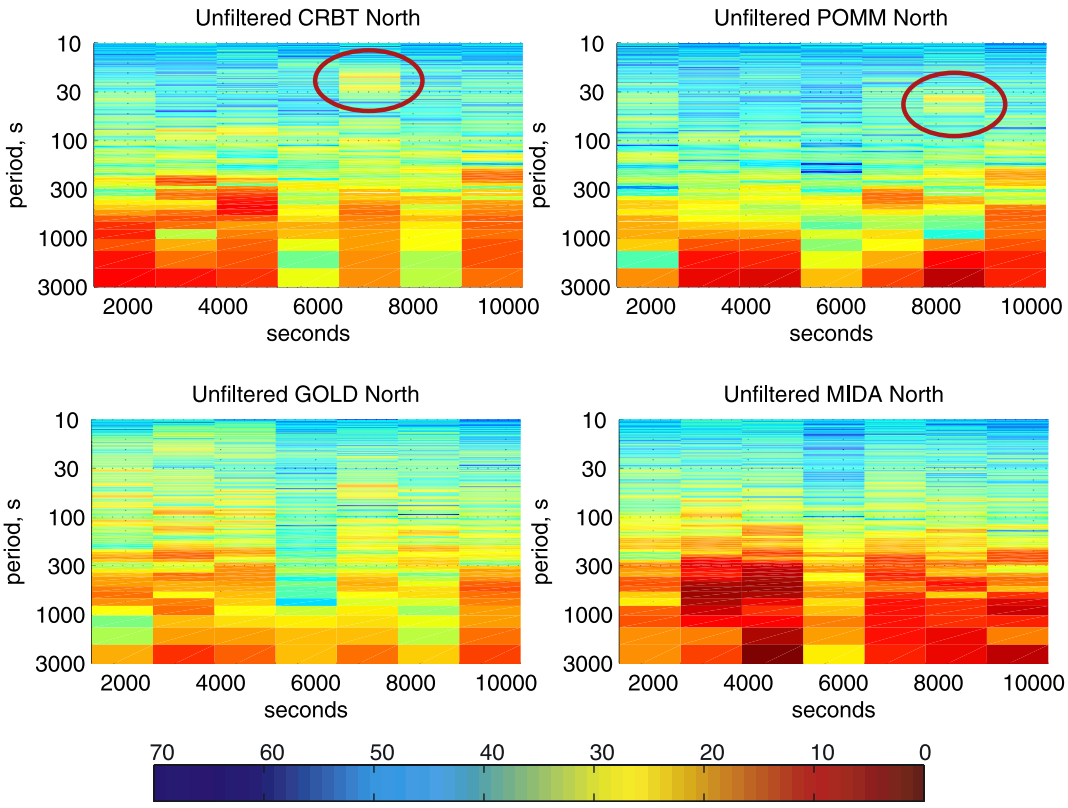

Figure 2. North component spectrograms for CRBT, POMM, GOLD, and MIDA, 26 September 2004, 1520 UTC. The transient short-period multipath is circled in red. The scale bar gives power units in m^2/Hz in dB.

GPS site and then describe and evaluate a method that removes multipath errors.

3. Multipath

[9] GPS multipath occurs when the transmitted signal arrives at an antenna via an indirect path rather than along the direct path. In the context of this study, multipath is caused by reflections from objects near the receiving antenna. A multipathed signal has a longer path length than a direct signal, introducing error to the pseudorange and carrier phase measurements, which then propagate into position solutions based on these data. Multipath may be either diffuse or specular in nature. Specular multipath is problematic because it produces systematic, time-correlated errors that are not easily treated by traditional analysis methods. In contrast, diffuse multipath takes on an unbiased, random appearance and is more easily removed through filtering within the receiver hardware. Various approaches for multipath reduction and correction have been developed. In summary, one can avoid or reduce susceptibility to reflected signals [*van Nee*, 1992; *Van Dierendonck et al.*, 1993; *Schupler and Clark*, 2001], calibrate or evaluate the errors using assumptions of spatial repeatability [*Cohen and Parkinson*, 1991], or estimate the multipath corrections from SNR data [*Axelrad et al.*, 1996; *Comp and Axelrad*, 1998]. Modeling approaches that use repeating orbital characteristics of the GPS constellation have also been suggested [*Genrich and Bock*, 1992; *Ge et al.*, 2000b; *Choi et al.*, 2004]; a new implementation of this methodology is discussed in section 4.

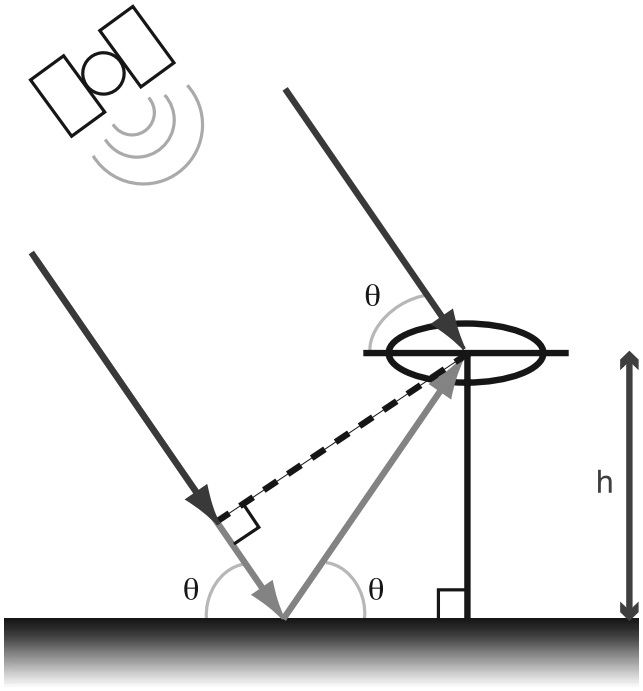

Figure 3. Multipath geometry for a standard GPS monument. For an infinite horizontal reflector such as the ground (shaded) the important parameters are the height (h) of the antenna above the ground and the satellite elevation angle (θ). These can be related to the additional path length (grey arrows) of a reflected signal.

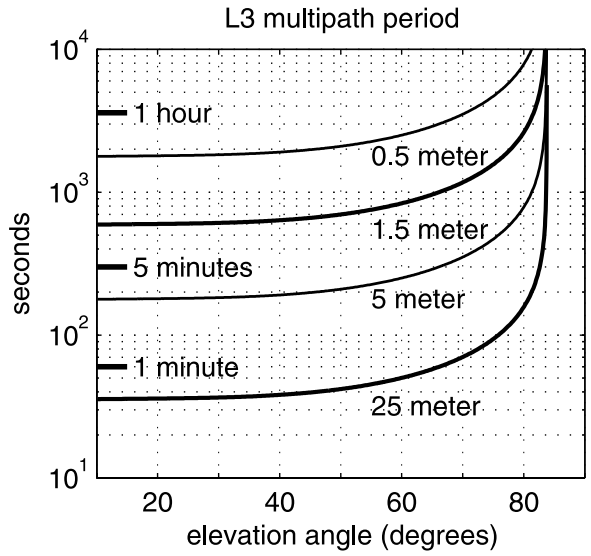

Figure 4. Period of L3 (ionosphere-free combination of L1 and L2) multipath errors for horizontal reflectors located at various distances (0.5, 1.5, 5, and 25 m) below the GPS antenna phase center at station POMM using the elevation history of the PRN6.

[10] The most straightforward multipath case involves specular multipath where the GPS antenna is located above an infinite horizontal reflector such as the ground (Figure 3). The time-dependent signature of multipath can best be understood by analyzing the frequencies inherent in multipath errors; discussion in the rest of this section involves only carrier phase multipath errors since the more precise carrier phase data are of greater interest to geodesists than pseudorange measurements. For GPS carrier phase multipath these frequencies can be expressed as a function of the relative phase (ψ), i.e., the phase difference between the direct and reflected signals. The parameters that determine the effect of reflected signals on the phase are the height of the antenna above the reflecting surface (h), the L1 or L2 GPS wavelength (λ), the satellite-receiver elevation angle (θ), and the reflecting characteristics of the horizontal surface (defined as the ratio (α) of the reflected signal amplitude with respect to the direct signal). For the specific case of a reflection from a horizontal surface the additional path length with respect to the direct signal (δ) was shown by *Georgiadou and Kleusberg* [1988]:

$$\delta = 2h \sin\theta \tag{1}$$

The corresponding relative phase and its time derivative are defined as

$$\psi = 2\pi\frac{\delta}{\lambda} + \psi_o = \frac{4\pi h}{\lambda}\sin\theta + \psi_o \tag{2}$$

$$\frac{d\psi}{dt} = \frac{4\pi h}{\lambda}\cos\theta\frac{d\theta}{dt}, \tag{3}$$

where ψ_o is a possible bias.

[11] Converting the phase delay rate to the period for a rising pass of a GPS satellite, Figure 4 summarizes multipath frequencies for a variety of horizontal reflector distances (0.5, 1.5, 5.0, and 25 m). One can discern two major features of GPS multipath. First, reflections from a horizontal surface will generate multipath oscillations with shorter periods at low satellite elevation angles than at high-elevation angles. Additionally, the gain pattern of most GPS antennas results in larger α at low-elevation angles than at high-elevation angles. Thus, for high-rate GPS applications at seismic frequencies, removing multipath at low elevations (where magnitudes are large and periods are short) will be of greater importance than at higher elevations. Second, close horizontal reflectors produce longer-period oscillations, and far horizontal reflectors produce shorter-period oscillations. For large antenna heights the oscillations at low elevations will be close to the period of seismic surface waves (20 s). These simple calculations explain why the GOLD spectrogram (Figure 2) showed significant energy at short periods: GOLD is attached to a tower $\sim$25 m above the ground. In contrast, CRBT has its antenna mounted $\sim$1.8 m above the ground and has a spectral signature dominated by the longer periods (Figure 2). The large long-period high noise levels at MIDA are believed to be caused by multipath from a tree. The transient short-period multipath signals seen at POMM and CRBT are not caused by an infinite horizontal reflector but more likely by a distant tilted surface that impacts only certain sections of the sky. More complicated derivations are required to understand the frequency of multipath reflections from a tilted surface [*Bilich*, 2006] and are not given here. Overall, reflections from distant surfaces (horizontal or tilted) have the potential to generate multipath at frequencies similar to that of seismic waves. While much of the early research on multipath at geodetic sites focused on near reflectors [e.g., *Elósegui et al.*, 1995], Figures 2 and 3 make it clear that properly correcting for far reflectors will be especially important for high-rate GPS applications where short-period phenomena are of significant interest. Section 4 describes how the daily repeatability of GPS orbits can be exploited to mitigate the effects of both short- and long-period multipath.

4. Aspect Repeat Time

[12] The repeatability of multipath is contingent on the repeatability of geometric relationships between the satellite, receiving antenna, and the surrounding environment. If one can establish the period at which geometric relationships will repeat, a multipath correction profile can be constructed from data collected on a day without significant displacements. With an appropriate time shift to align geometric repeatability the multipath correction profile can be applied to another day when actual displacements occur. A key assumption is that the ground did not move on the correction profile day, and thus changes in the position estimates represent a combination of high-frequency random error (removed by low-pass filtering) and systematic errors caused by multipath and any other error that repeats with the satellite geometry. An example time series demonstrating this method is shown in Figure 5. The remaining long-period errors can be largely removed by stacking [*Wdowinski et al.*, 1997], as will be discussed in section 6. While the overall success of this method relies on the

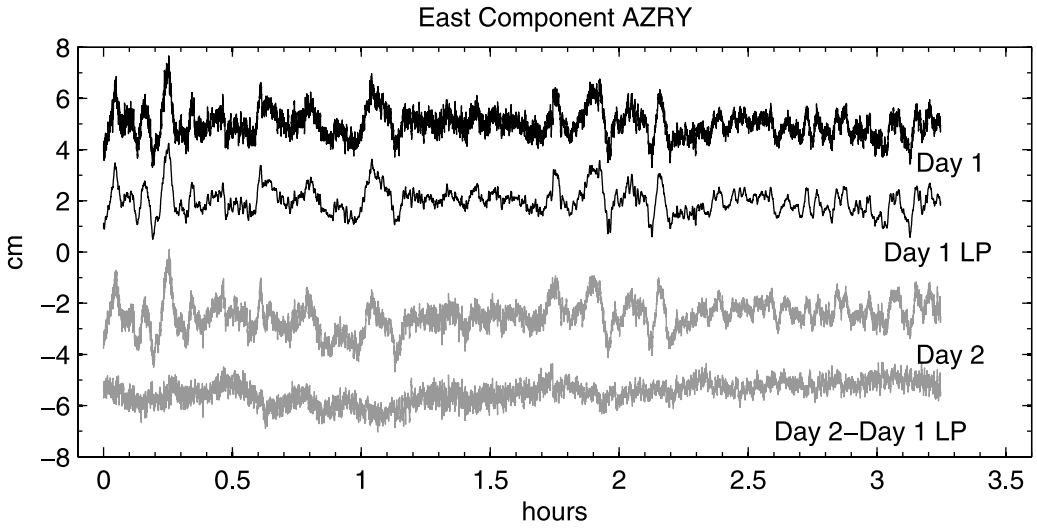

Figure 5. Error reduction stages for high-rate (1 Hz) position estimates, east component of AZRY. The original 1-Hz position estimates (top trace) are shifted forward by the average orbit repeat time then low-pass (LP) (11 s) filtered (second trace). Subtracting the first day LP-filtered positions from the 1-Hz position estimates for the second day (third trace) reduces the errors in positions (fourth trace).

geometric repetition of the satellite orbits, another important assumption is that the reflectance is the same between days, i.e., α is constant.

[13] Since the GPS orbital period and therefore the geometry of a GPS satellite with respect to an antenna repeats at approximately a sidereal period (236 s less than 1 day), multipath effects will also repeat at approximately this period. *Genrich and Bock* [1992] were the first to recommend that the "sidereal" satellite repeat time be used to account for multipath effects. *Choi et al.* [2004] subsequently pointed out that the sidereal shift period used by *Genrich and Bock* [1992] was off by ~9 s. Following the discussion by *Choi et al.* [2004], it can be shown that each GPS satellite has a distinct orbit repeat period which itself varies by ~8 s throughout the year. Furthermore, satellites being maneuvered can differ from the sidereal orbit repeat period by over 100 s. The inherent variability of GPS satellite orbits and their respective geometric repeat times must be taken into account for proper implementation of "modified sidereal filtering."

[14] The repetition of the satellite ground track [*Axelrad et al.*, 2005; *Larson*, 2005; *Agnew and Larson*, 2007] gives a much better proxy for multipath repeatability than the GPS orbital repeat period because a signal from a GPS satellite with a closely repeating ground track will reflect off the same obstacles on the ground. *Agnew and Larson* [2007] use an astronomical term, aspect, to describe the time when the satellite comes closest to occupying the same topocentric place and thus a repeating ground track. In order to eliminate ongoing references to the incorrect shift period (sidereal and modified sidereal) for describing this multipath mitigation technique we will use aspect repeat time adjustment (ARTA) to describe our new implementation.

[15] For most GPS satellites the orbit repeat period and the aspect repeat period agree very well. As a GPS satellite deviates from the ideal orbital repeat period (1 day minus ~245 s) the correspondence between the orbit repeat period and the ground track repeat period breaks down. How variable is the aspect repeat time for the GPS constellation? Figure 6 summarizes both orbit and aspect repeat periods

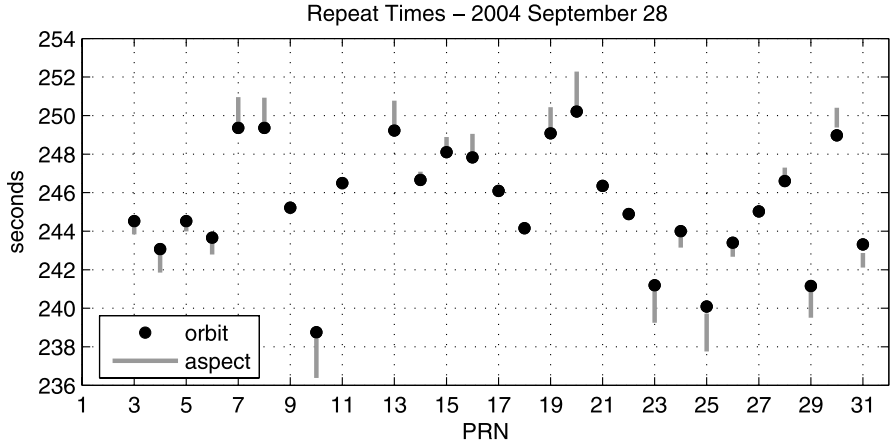

Figure 6. Orbit repeat times and variations in aspect repeat times calculated for 28 September 2004 at Parkfield, California. The aspect repeat time for PRN 1 varies from 298 to 318 s; its orbit repeat time is 297 s.

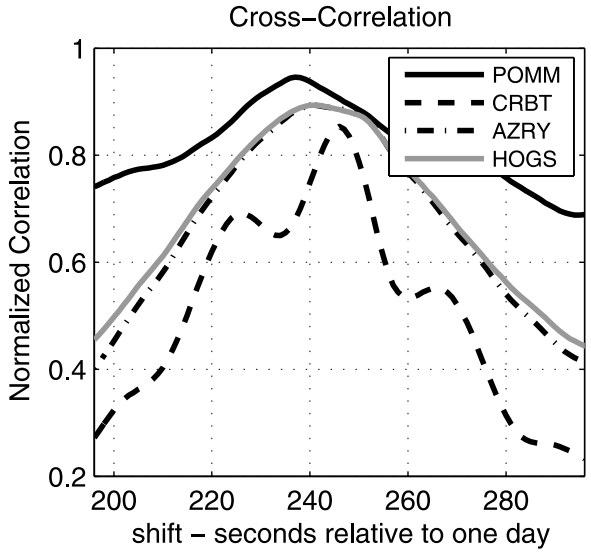

Figure 7. Normalized cross correlations for the north component of SCIGN sites POMM, AZRY, HOGS, and CRBT for 25 and 26 September 2004, 1645–1800 UTC.

for our study period. Note how the variation in aspect repeat time always extends away from the orbit repeat time. The magnitude of that variation is larger depending on how far the satellite deviates from the ideal orbital repeat period. For example, the aspect repeat time for PRN 17 (orbit repeat period of 1 day minus 246 s) varies by no more than 0.14 s, whereas the aspect repeat time for PRN 25 (orbit repeat period of 1 day minus 240 s) varies by more than 2 s. The practical consequence of this variation is that any implementation of ARTA that uses PRN 25 data must allow its repeat time to vary within a single-satellite pass by 2 s. While this is a small variation, if PRN25 creates multipath errors with reflections far from the antenna, the period of multipath errors will be short, with 2 s representing a significant fraction of the oscillation period. Inadequately accounting for multipath error such as this will produce degraded ARTA results. Not shown in Figure 6 are the aspect repeat times for PRN 1 on 28 September 2004. This satellite was very far from the ideal orbital repeat period and thus has a very large variation (~20 s) over a satellite pass. The separation of the repeating ground tracks for this satellite is more than 30 km. For the purposes of ARTA, satellites like PRN 1 should not be used in high-rate GPS analyses.

5. Position Repeat Time and Implementation

[16] Although it is straightforward to compute the aspect repeat time for an individual satellite (software is available at http://www.ngs.noaa.gov/gps-toolbox/), since multiple satellites contribute to each position estimate, it is not obvious which time shift to use for high-rate positions. Furthermore, since we expect low-elevation satellites to contribute more multipath error to a position solution, it is likely that lower-elevation angle satellites should be more heavily weighted in determining the position shift time. As pointed out by *Choi et al.* [2004], as different satellites rise and set, the position time shift will vary. Since the noise characteristics of different sites shown in Figure 2 vary significantly in frequency and amplitude, it would not be surprising to also find that different sites require different time shifts.

[17] A cross correlation was computed to determine the optimal position shift for a few of the GPS sites in our study area (Figure 7) to demonstrate this variation. Most of the sites in our study area are like HOGS and AZRY; they have broad correlation peaks centered at ~245 s less than 1 day. In contrast, POMM has a peak at a much shorter time shift (237 s), and CRBT has a very sharp cross-correlation peak centered at 246 s. The peaks at CRBT and POMM are correlated with the transient high-frequency energy shown in Figure 2. Inspection of solution postfit residuals and SNR data indicated that the high-frequency energy was caused by different satellites at the two sites: PRN 25 (POMM) and PRN 11 (CRBT). The two peaks in the position time series correspond with the aspect repeat period for those individual satellites at these specific times. Since the POMM oscillations occurred during the Parkfield earthquake rupture, minimizing these errors was of particular interest.

[18] We examined two ways to determine optimal shifts for position time series: using the peak cross correlation or minimizing the RMS difference for a range of shifts (e.g., 236–256 s). Figure 8 shows cross correlations calculated for twenty-four 500-s time intervals. In general, the RMS improvement method (shown as circles) agrees well with the maximum cross-correlation values. When there is a broad maximum cross correlation, the two techniques may differ by 1 or 2 s. In a few of the solutions, there are multiple cross-correlation peaks; in some of these cases the RMS improvement method chose the second largest cross-correlation peak. We compared time series for these cases with shifts determined by maximizing the RMS improvement; in each case the RMS improvement method did a better job of improving the time series at high frequencies. For future discussion we have used RMS improvement as the metric to define the optimal time shift.

[19] How often a shift interval needs to be estimated depends on how often the dominant multipath period changes. In Figure 9 the RMS is computed in each consecutive time interval for a 3.3-hour period, using intervals of 250–1500 s. The longer intervals (1000–1500 s) are clearly worse than using the shorter (250–750 s) intervals. Although the 250-s interval gives consistently low RMS values, they are also highly variable. When we examined the estimated shift values associated with a 250-s interval, we noted they were also physically implausible, e.g., estimated shift values oscillated by 10 s. A 500-s time interval is used in this study as it provides good RMS improvement and avoids nonphysical oscillatory behavior.

[20] For a multipath environment to repeat in a GPS position time series it is important that the same satellites contribute to each position solution involved in the ARTA process [*Bilich*, 2006]. This condition is not generally met using existing GPS analysis software packages. The simplest example of this failure is when a different set of satellites is used by the software package on two consecutive days, although the same set of satellites might have been transmitting a signal on each day. This failure to track the same satellites on two consecutive days can be at the receiver level but is also frequently caused by data editing

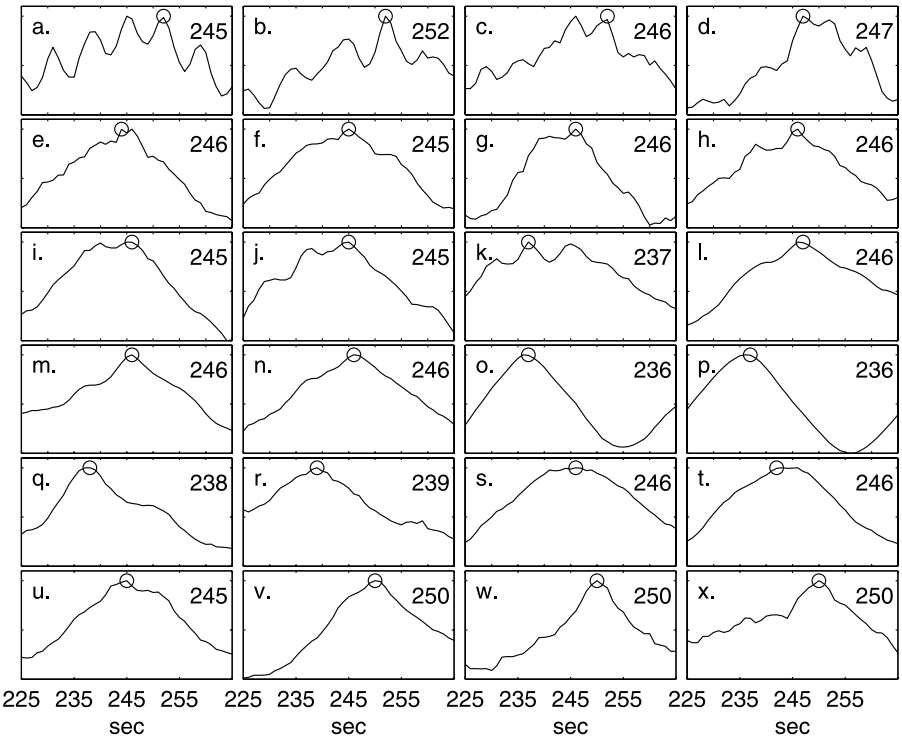

Figure 8. (a–x) Cross-correlation (normalized, with *y* axis labels removed for clarity) time shifts for 500-s increments for north component POMM positions on 25 and 26 September 2004, 1520–1840 UTC. Peak cross-correlation time shifts are given in the top right (seconds defined relative to 1 day). The circles depict the best shift value, determined by minimizing the RMS difference of the two time series.

[*Blewitt*, 1990]. Figure 10 demonstrates the impact of "unequal" satellite sets on the success of ARTA. High-rate positions were estimated for a 3.3-hour period for GPS site HOGS on 3 days and shifted by the ideal orbit repeat period. Figure 10a shows the difference of shifted position estimates for three pairs of solutions. While most of the position differences appear to be randomly distributed, in the first hour of the time series, there are large systematic variations. Figure 10b examines this period in more detail with undifferenced solutions. The largest discrepancies between the three solutions correlate with times when the number of satellites in a given solution varied (Figure 10c). Furthermore, positions computed at times later in the hour agree well when the same number of satellites was used on each day. In order to achieve the best implementation of ARTA it is necessary to preedit the data files to equalize the satellites viewed on each day. For the remainder of this paper it is assumed that the observable files have been edited to ensure the same satellites are observed on each day.

[21] In addition to a common number of observations the best ARTA implementation also requires that each solution have a common number of estimated parameters. In an example from the GPS site RNCH (Figure 11a), position solutions on two consecutive days differ only by a large offset on the second day. This correlates with an additional phase ambiguity at RNCH for PRN 20. Because only 24 min of data are available after this phase ambiguity, GIPSY was unable to resolve it. In Figure 11b, new RNCH solutions are shown where the same 24 min of PRN20 data have been removed on both days, and the extra phase ambiguity is no longer necessary. The apparent offset is now significantly reduced. An alternative way to equalize the RNCH position solutions would be to add an extra phase ambiguity on the first day.

[22] Least squares solution residuals are an alternate data type for generating multipath correction profiles. In this study we have opted to shift position time series, as

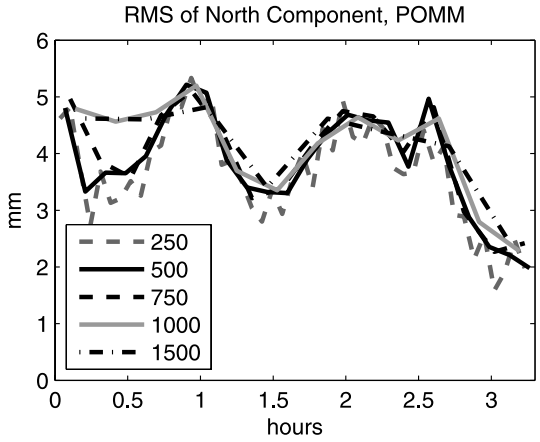

Figure 9. RMS for north component position estimates at GPS site POMM after aspect repeat time adjustment (ARTA) using time series of length 250, 500, 750, 1000, and 1500 s. Time is defined relative to 1520 UTC, 26 September 2004.

was originally suggested by *Genrich and Bock* [1992], because of the flexibility of using positions over residuals. In testing these two implementations (residual shifting and position shifting) of ARTA we found excellent agreement at the longer periods (100–1000 s) but found that tuning the shifts using the position time series did a better job at removing multipath at short periods (20–50 s). One advantage of using residuals is that only a single extra day is needed to create a multipath correction profile. Our ARTA implementation requires 2 days in order to estimate the optimal shifts for the multipath correction profile.

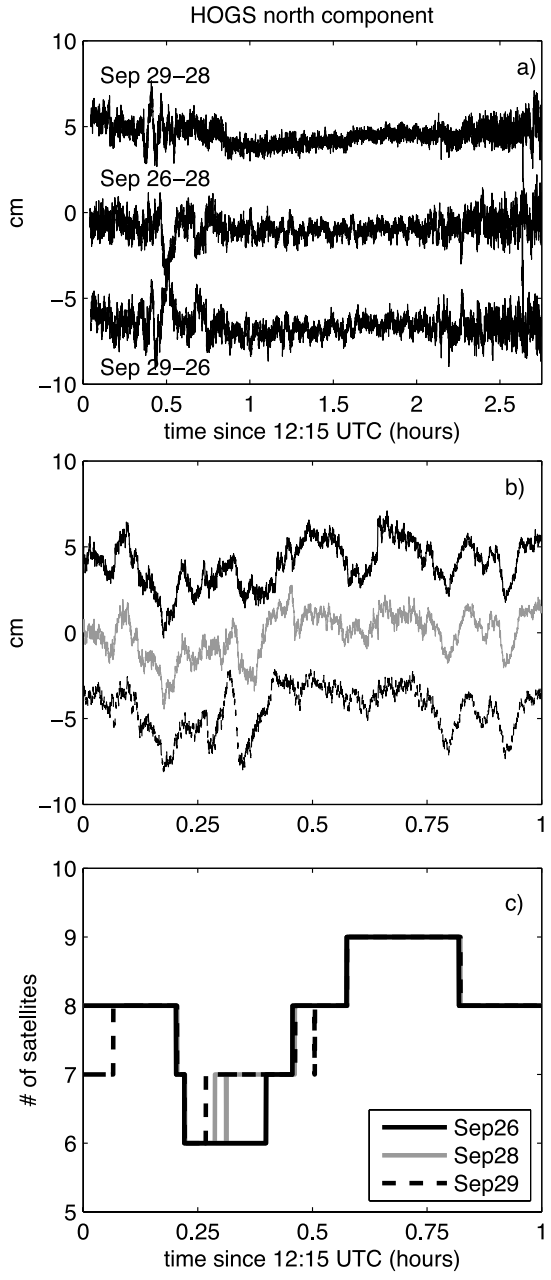

Figure 10. (a) Difference of north position estimates for station HOGS on 26, 28, and 29 September (data from 27 September had significant gaps at multiple sites). (b) Close-up view of undifferenced position estimates for 26, 28, and 29 September. (c) Number of satellites used in each solution.

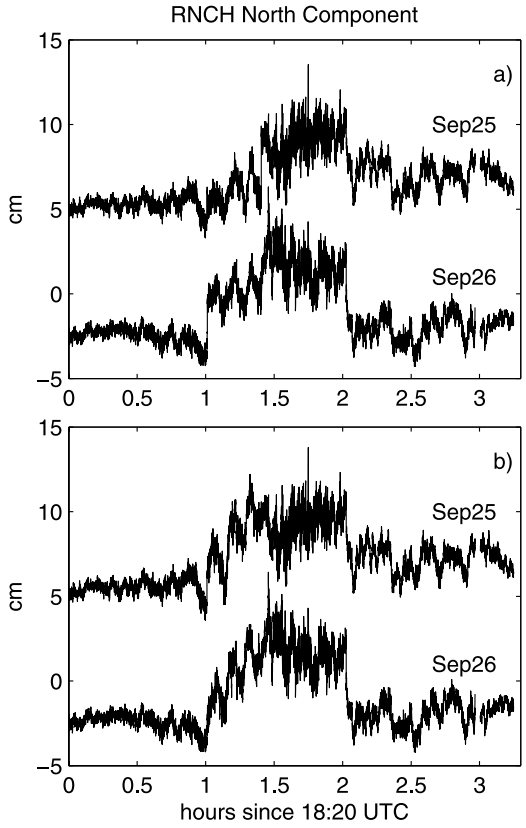

Figure 11. (a) RNCH north position estimates on 25 and 26 September 2004. An unresolved phase ambiguity on PRN20 occurs at hour 1 and results in a sharp jump in the 26 September series. (b) RNCH solutions where 24 min of PRN20 data have been removed.

6. Results

[23] We return to POMM and CRBT to examine position precision improvements in the spectral domain after implementing ARTA as described in section 5. In particular, by comparing Figure 2 (raw positions) to Figure 12 (after ARTA), improvements are achieved in two different spectral and temporal ranges: at long periods over the entire position time series and at short periods for isolated sections of the time series. The long periods correspond to reflections from ~2-m horizontal reflectors such as the ground underneath the antenna, and the latter correspond to multipath (20–50 s) caused by far reflectors of less widespread extent. The improved post-ARTA north positions for POMM and CRBT are provided in Figure S5 in the auxiliary material[1].

[24] The post-ARTA spectrograms for CRBT and POMM show long-period (>1000 s) errors that vary in time and appear to have common amplitudes. While some of this error is due to unmodeled multipath at the reference site [*Bilich*, 2006], some originates with any unmodeled error that affects all sites simultaneously. Stacking and removing

[1]Auxiliary materials are available in the HTML. doi:10.1029/2006JB004367.

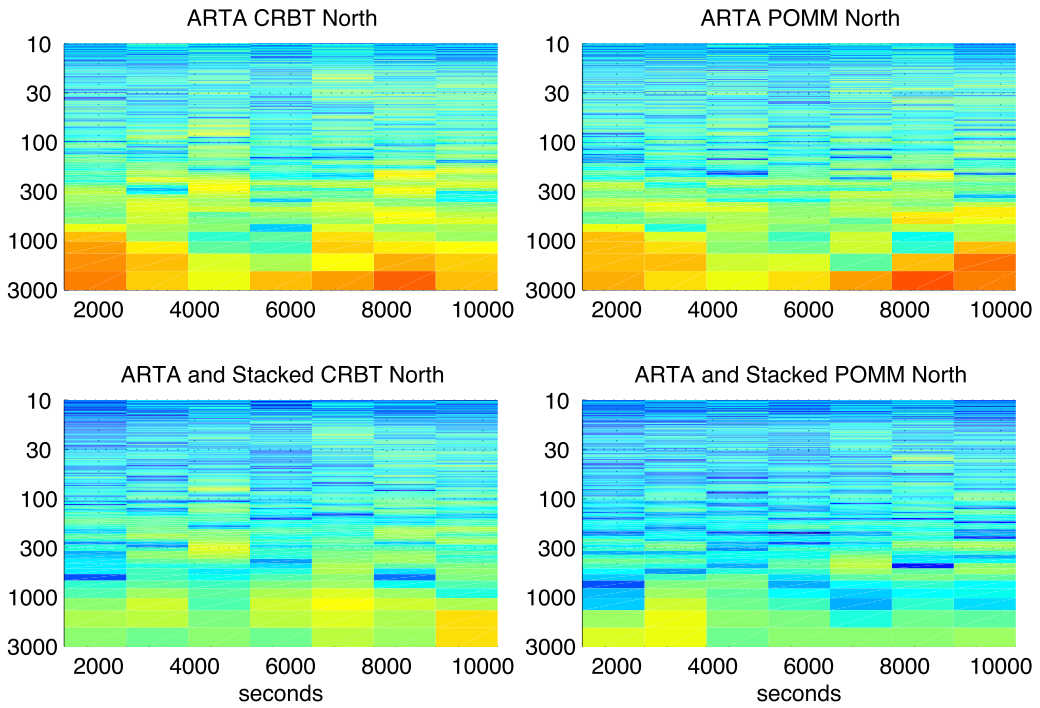

Figure 12. North component spectrograms for CRBT and POMM after ARTA processing and stacking, with periods (in seconds) on the *y* axis. The scale bar is given in Figure 2.

these common mode errors is analogous to the technique introduced by *Wdowinski et al.* [1997] to remove errors in 24-hour averaged positions. The "stack" or time-varying empirical correction is calculated by averaging positions for network sites outside the region of active deformation. For example, since Parkfield is the region of interest, sites such as FVPK, AZRY, DHLG, WHYT, and KYVW (more than 350-km distant) are used to create the stack, which is subsequently subtracted from the Parkfield position estimates. Figure 12 also provides spectrograms after stacking, demonstrating that while precision is improved at all frequencies, the most dramatic improvement is at long periods.

[25] In order to summarize the noise characteristics of high-rate GPS we calculated the power spectra for four separate 3.3-hour periods, using overlapping segments and a Hanning taper (Figure 13). Each spectrum shown is the average of the spectra computed for the eight SCIGN sites (Figures S1–S7 in the auxiliary material). We compare our results with the recent *Langbein and Bock* [2004] (hereinafter referred to as LB2004) study of 1-Hz positioning errors for GPS sites in the Parkfield array. There are several key differences between these studies. LB2004 summarized relative positioning precision estimates for short baselines; in this study, positions are determined in the ITRF2000 reference frame. LB2004 used a nonoptimal shift period (1 day minus 236 s) for modeling multipath; we allowed the shift period to vary by site and time. Finally, LB2004 used a real-time processing system, whereas the positions in our paper were computed after the fact. To compare results, we used a fit to their network power spectra results (Table 1 in LB2004) for periods less than an hour. Both LB2004 and this study show that high-rate GPS noise spectra follow 1/frequency. Although our results are better at short periods (<10 s), this is entirely because of stacking, a methodology that was not implemented in LB2004. At longer periods the improved precision with respect to LB2004 is due to both ARTA and stacking, with our ARTA implementation providing better improvement at periods less than 1000 s. By showing spectra for separate time periods we emphasize that noise characteristics for high-rate GPS vary significantly throughout the day as the geometric strength of the GPS constellation changes; for example, during the worst period (1820 UTC), high-noise positions correlate with large formal errors (Figure S7). Note in particular the spread in north component precision at all periods. East component precision is more consistent, with some divergence at the longer periods.

7. Discussion

[26] The methodologies described here can easily be applied in near-real time to continuously operating 1-Hz GPS stations using noncommercial geodetic-quality software. Nevertheless, simple software improvements could be made to improve high-rate GPS data analysis. For example, data-editing modules sometimes have fixed parameters that assume receivers are sampling at 30 s; this should be rethought for 1 s and higher receiver sampling rates. Likewise, data-editing software optimized for ionospheric characteristics at midlatitudes sometimes performs poorly for very high and low latitude stations; the 1-Hz data rate should make it easier to differentiate between cycle slips and ionospheric variability. Additional study is needed to evaluate high-rate vertical precision where trade-offs with troposphere estimation strategies are important. Further, while this study used precise IGS ephemerides that are generally available a week later, equivalent results are likely

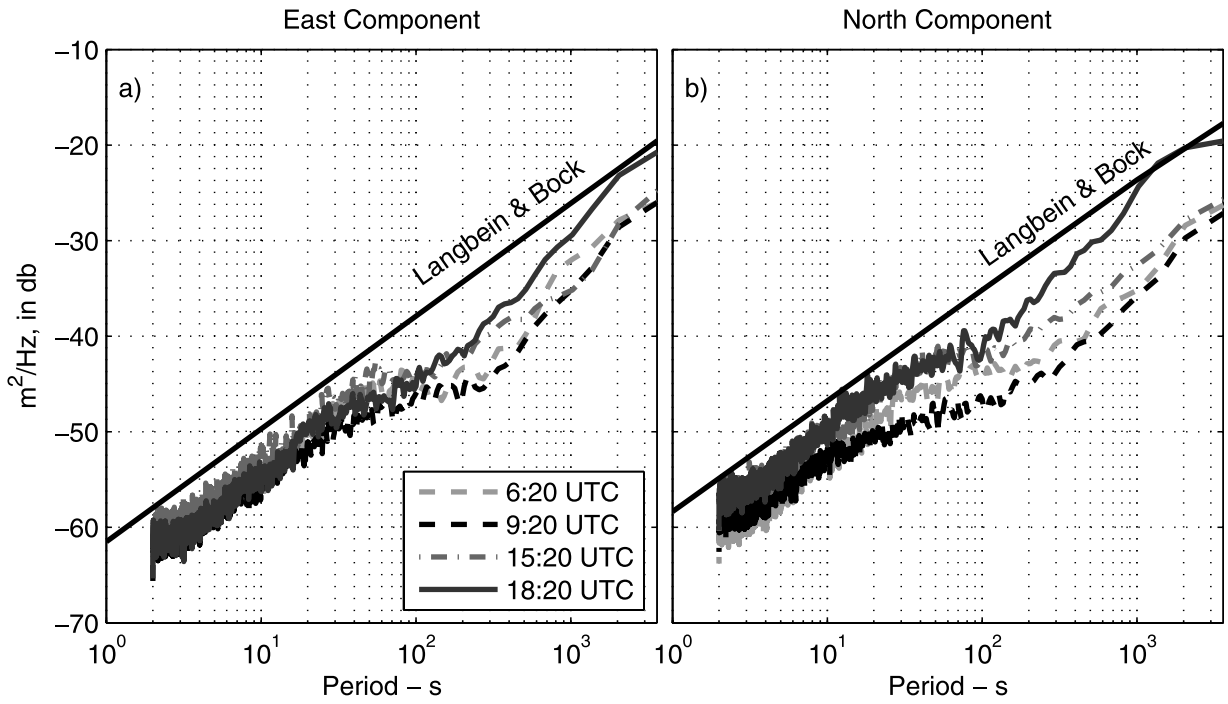

Figure 13. (a) East and (b) north component average-power spectra for four 3.3-hour periods compared with *Langbein and Bock*'s [2004] estimates (straight line). Network data from 1220 UTC are not presented because of significant data outages.

to be obtained using the very high quality rapid IGS ephemerides available within 24 hours.

[27] It is more difficult to assess how easily these methods can be implemented in real time. While ultrarapid (http://www.gfz-potsdam.de/pb1/igsacc/igsacc_ultra.html) IGS ephemerides are much more accurate than broadcast ephemerides, because they are based on prediction rather than postanalysis, they will always be less accurate than precise or rapid ephemerides. With predicted orbits, estimated positions from smaller aperture networks like Parkfield will always be more accurate than for the larger networks shown here.

[28] As disk storage and memory have become less expensive, many continuous GPS receivers are being converted to operate at 1 Hz. Nevertheless, there will always be data of interest to geophysicists that were collected at lower sampling rates, e.g., 30 s. While these GPS data are not useful for seismic applications, they are of significant interest for monitoring volcanic activity and postseismic deformation. For future research we plan to investigate how to reduce multipath errors in GPS time series at periods appropriate to these data sets (minutes to hours).

8. Conclusions

[29] The theory and sample results presented here illustrate the key factors in correcting site-specific multipath for high-rate GPS applications. The primary limitations are the level of repeatability of the GPS satellite orbits and the frequency of the multipath oscillations. These two factors couple together in that successful reduction of short-period multipath effects is sensitive to the degree of repetition of the GPS satellite ground track. In order to accurately estimate dynamic displacements at seismic frequencies with GPS, multipath errors with periods of 20–50 s caused by far multipath reflectors must be reduced.

[30] Recognizing that satellites do not contribute equally to position estimates and have disparate levels of multipath, a new implementation of ARTA has been developed. Optimal shift periods are estimated from the position time series for each GPS site and are allowed to vary in time to accommodate changes in the multipath environment. If available, stations outside the area of geophysical interest can be used to model common mode errors. Using 12 hours of 1-Hz GPS data from southern California, the standard deviation of east and north component positions were improved from 6.2 to 2.6 mm and 8.2 to 3.0 mm, respectively.

[31] **Acknowledgments.** This research was sponsored by NSF grants on multipath (EAR-0003943) and high-rate GPS (EAR-0337206), a NSF graduate student research fellowship (A.B.), a CU Faculty Fellowship (K.M.L.), and a USGS grant (05HQGR0015). Infrastructure support for GPS research in the United States is provided by UNAVCO, JPL, NASA, IGS, and SOPAC. All SCIGN (W.M. Keck Foundation, NASA, NSF, USGS, and SCEC) data are in the public domain. GIPSY was developed and licensed by JPL. Mark Simons and Geoff Blewitt encouraged us to estimate optimal shifts from the time series themselves. Duncan Agnew provided useful feedback on an earlier draft of the manuscript and wrote the asprep code that is available at the GPS Tool Box (available at http://www.ngs.noaa.gov/gps-toolbox/). Orbit repeat period software is also available at that Web site. We thank Kyuhong Choi, Stephen Esterhuizen, James Gidney, John Berg, George Rosborough, and Michael Scharber. We also thank an anonymous reviewer and Jan Kouba for helpful review comments that substantially improved this manuscript.

References

Agnew, D. C. (1992), The time-domain behavior of power-law noises, *Geophys. Res. Lett.*, *19*(4), 333–336.

Agnew, D. C., and K. M. Larson (2007), Finding the repeat times of the GPS constellation, *GPS Solutions*, *11*(1), 71–76.

Altamimi, Z., P. Sillard, and C. Boucher (2002), ITRF2000: A new release of the International Terrestrial Reference Frame for earth science applications, *J. Geophys. Res.*, *107*(B10), 2214, doi:10.1029/2001JB000561.

Axelrad, P., C. Comp, and P. MacDoran (1996), SNR based multipath error correction for GPS differential phase, *IEEE Trans. Aerosp. Electron. Syst.*, *32*(2), 650–660.

Axelrad, P., K. Larson, and B. Jones (2005), Use of the correct satellite repeat period to characterize and reduce site-specific multipath errors, in *Institute of Navigation Global Navigation Satellite Systems 2005 Proceedings*, pp. 2638–2648, Inst. of Navig., Fairfax, Va.

Beutler, G., I. I. Mueller, and R. E. Neilan (1994), The international GPS service for geodynamics (IGS): Development and start of official service on January 1, 1994, *Bull. Geod.*, *68*(1), 39–70.

Bilich, A. (2006), Improving the precision and accuracy of geodetic GPS: Applications to multipath and seismology, Ph.D. dissertation, Univ. of Colo., Boulder.

Blewitt, G. (1989), Carrier phase ambiguity resolution for the Global Positioning System applied to geodetic baselines up to 2000 km, *J. Geophys. Res.*, *94*, 10,187–10,203.

Blewitt, G. (1990), An automatic editing algorithm for GPS data, *Geophys. Res. Lett.*, *17*(3), 199–202.

Bock, Y., R. Nikolaidis, P. de Jonge, and M. Bevis (2000), Instantaneous geodetic positioning at medium distances with the Global Positioning System, *J. Geophys. Res.*, *105*, 28,223–28,253.

Bock, Y., L. Prawirodirdjo, and T. I. Melbourne (2004), Detection of arbitrarily large dynamic ground motions with a dense high-rate GPS network, *Geophys. Res. Lett.*, *31*, L06604, doi:10.1029/2003GL019150.

Celebi, M., W. Prescott, R. Stein, K. Hudnut, J. Behr, and S. Wilson (1999), GPS monitoring of dynamic behavior of long-period structures, *Earthquake Spectra*, *15*(1), 55–66.

Choi, K., A. Bilich, K. M. Larson, and P. Axelrad (2004), Modified sidereal filtering: Implications for high-rate GPS positioning, *Geophys. Res. Lett.*, *31*, L22608, doi:10.1029/2004GL021621.

Cohen, C. E., and B. W. Parkinson (1991), Mitigating multipath in GPS-based attitude determination, *Adv. Astronaut. Sci.*, *74*, 53–68.

Comp, C., and P. Axelrad (1998), Adaptive SNR-based carrier phase multipath mitigation technique, *IEEE Trans. Aerosp. Electron. Syst.*, *34*(1), 264–276.

Elósegui, P., J. L. Davis, R. K. Jaldehag, J. M. Johansson, A. E. Niell, and I. I. Shapiro (1995), Geodesy using the Global Positioning System: The effects of signal scattering on estimates of site position, *J. Geophys. Res.*, *100*, 9921–9934.

Elósegui, P., J. L. Davis, D. Oberlander, R. Baena, and G. Ekström (2006), Accuracy of high-rate GPS for seismology, *Geophys. Res. Lett.*, *33*, L11308, doi:10.1029/2006GL026065.

Emore, G., J. Haase, K. Choi, K. M. Larson, and A. Yamagiwa (2007), Recovering absolute seismic displacements through combined use of 1-Hz GPS and strong motion accelerometers, *Bull. Seismol. Soc. Am.*, *97*(2), 357–378, doi:10.1785/0120060153.

Ge, L. (1999), GPS seismometer and its signal extraction, in *12th International Technical Meeting of the Satellite Division of the Institute of Navigation*, pp. 41–52, Inst. of Navig., Fairfax, Va.

Ge, L., S. Han, C. Rizos, Y. Ishikawa, M. Hoshiba, Y. Yoshida, M. Izawa, N. Hashimoto, and S. Himori (2000a), GPS Seismometers with up to 20 Hz Sampling Rate, *Earth Planets Space*, *52*(10), 881–884.

Ge, L., S. Han, and C. Rizos (2000b), Multipath mitigation of continuous GPS measurements using an adaptive filter, *GPS Solutions*, *4*(2), 19–30.

Genrich, J. F., and Y. Bock (1992), Rapid resolution of crustal motion at short ranges with the Global Positioning System, *J. Geophys. Res.*, *97*, 3261–3269.

Georgiadou, Y., and A. Kleusberg (1988), On carrier signal multipath effects in relative GPS positioning, *Manuscr. Geod.*, *13*, 172–179.

Hudnut, K. W., Y. Bock, J. E. Galetzka, F. H. Webb, and W. H. Young (2002), The southern California integrated GPS network (SCIGN), in *Seismotectonics in Convergent Plate Boundary*, edited by Y. Fujinawa and A. Yoshida, pp. 167–189, Terra Sci., Tokyo.

Ji, C., K. M. Larson, Y. Tan, K. W. Hudnut, and K. Choi (2004), Slip history of the 2003 San Simeon earthquake constrained by combining 1-Hz GPS, strong motion, and teleseismic data, *Geophys. Res. Lett.*, *31*, L17608, doi:10.1029/2004GL020448.

Kobayashi, R., S. Miyazaki, and K. Koketsu (2006), Source processes of the 2005 west off Fukuoka Prefecture earthquake and its largest aftershock inferred from strong motion and 1-Hz GPS data, *Earth Planets Space*, *58*, 57–62.

Kouba, J. (2003), Measuring seismic waves induced by large earthquakes with GPS, *Stud. Geophys. Geod.*, *47*, 741–755.

Langbein, J., and Y. Bock (2004), High-rate real-time GPS network at Parkfield: Utility for detecting fault slip and seismic displacements, *Geophys. Res. Lett.*, *31*, L15S20, doi:10.1029/2003GL019408.

Langbein, J., et al. (2005), Preliminary report on the 28 September 2004 *M*6.0 Parkfield, California earthquake, *Seismol. Res. Lett.*, *76*(1), 10–26.

Larson, K. (2005), Rising through the stack: Assessing the scientific value of high-rate GPS, *Eos Trans. AGU*, *86*(52), Fall Meet. Suppl., Abstract G13A-03.

Larson, K., P. Bodin, and J. Gomberg (2003), Using 1-Hz GPS data to measure deformations caused by the Denali Fault earthquake, *Science*, *300*, 1421–1424.

Lichten, S. M., and J. S. Border (1987), Strategies for high-precision Global Positioning System orbit determination, *J. Geophys. Res.*, *92*, 12,751–12,762.

Mattia, M., M. Rossi, F. Guglielmino, M. Aloisi, and Y. Bock (2004), The shallow plumbing system of Stromboli Island as imaged from 1 Hz instantaneous GPS positions, *Geophys. Res. Lett.*, *31*, L24610, doi:10.1029/2004GL021281.

Melbourne, T. I., and F. H. Webb (2002), Precursory transient slip during the 2001 M_w = 8.4 Peru earthquake sequence from continuous GPS, *Geophys. Res. Lett.*, *29*(21), 2032, doi:10.1029/2002GL015533.

Miyazaki, S., K. M. Larson, K. Choi, K. Hikima, K. Koketsu, P. Bodin, J. Haase, G. Emore, and A. Yamagiwa (2004), Modeling the rupture process of the 2003 September 25 Tokachi-Oki (Hokkaido) earthquake using 1-Hz GPS data, *Geophys. Res. Lett.*, *31*, L21603, doi:10.1029/2004GL021457.

Schupler, B., and T. Clark (2001), Characterizing the behavior of geodetic GPS antennas, *GPS World*, *12*, 48–55.

Segall, P., and J. L. Davis (1997), GPS applications for geodynamics and earthquake studies, *Annu. Rev. Earth Planet. Sci.*, *25*, 301–336.

Van Dierendonck, A. J., P. Fenton, and T. Ford (1993), Theory and performance of narrow correlator Spacing in a GPS Receiver, *Navigation*, *39*(3), 265–283.

van Nee, D. J. R. (1992), Reducing multipath tracking errors in spread-spectrum ranging systems, *Electron. Lett.*, *28*(8), 729–731.

Wang, G.-Q., D. Boore, G. Tang, and X. Zhou (2007), Comparisons of ground motions from colocated and closely spaced one-sample-per-second Global Positioning System and accelerograph recordings of the 2003 *M* 6.5 San Simeon, California, earthquake in the Parkfield region, *Bull. Seismol. Soc. Am.*, *97*(1B), 76–90.

Wdowinski, S., Y. Bock, J. Zhang, P. Fang, and J. Genrich (1997), Southern California permanent GPS geodetic array: Spatial filtering of daily positions for estimating coseismic and postseismic displacements induced by the 1992 Landers earthquake, *J. Geophys. Res.*, *102*, 18,057–18,070.

P. Axelrad, A. Bilich, and K. M. Larson, Department of Aerospace Engineering Sciences, University of Colorado, Boulder, CO 80309, USA. (Kristinem.Larson@gmail.com)